

Fluorinated Tetrathiafulvalenes with Preserved Electron-Donor Properties and Segregated Fluorous Bilayer Structures Based on F...F Nonbonded Interactions[†]

O. J. Dautel and M. Fourmigué*

"Sciences Moléculaires aux Interfaces", FRE 2068 CNRS-Université de Nantes, 2, rue de la Houssinière, BP32229, 44322 Nantes Cedex 3, France

marc.fourmigue@cnrs-immn.fr

Received April 5, 2000 (Revised Manuscript Received June 27, 2000)

The synthesis of the fluorinated 4,5-(2,2'-difluoropropylenedithio)-1,3-dithiol-2-one heterocycle with DAST allows for the preparation of several symmetrical and unsymmetrical di- and tetrafluoro-substituted tetrathiafulvalenes with accessible oxidation potentials ($0.6 < E^{1/2} < 0.85$ V vs SCE) despite the presence of the electron-withdrawing CF₂ groups. The flexibility of the fluorinated seven-membered ring identified from room-temperature NMR data has been thoroughly investigated by temperature-variable ¹H and ¹⁹F NMR experiments, allowing for the identification of two independent folding processes, whose coalescence temperatures (T_c) and activation energies (ΔG^\ddagger) were determined ($T_c = -15$ °C, $\Delta G^\ddagger = 50.2$ kJ mol⁻¹ and $T_c = 47$ °C, $\Delta G^\ddagger = 51.1$ kJ mol⁻¹). The analysis of the X-ray crystal structures of three of those fluorinated TTF demonstrates the efficiency of the nonbonded fluorine exclusion interactions for the stabilization of layered structures with fluorous bilayers, together with S...S van der Waals interactions and C–H...F hydrogen bonds.

Introduction

Fluorine/fluorine interactions play an unique role precisely because they are very weak if not negligible. This behavior originates in the low polarizability of the fluorine atom that leads to limited attractive interatomic dispersion forces.¹ The consequences of these low attractive forces have been studied in the liquid phase, fluorocarbons have been indeed described as the least associated liquids,² comparable in that respect to gases, which actually dissolve extremely well in them. This property has been exploited for applications in the biomedical field, such as oxygen transport and liquid ventilation.² Amphiphilic molecules which incorporate both aliphatic and fluorinated fragments have been shown to organize into thermotropic smectic phases,³ lyotropic micellar systems^{2,4,5} or bilayers⁶ where the two types of fragments segregate. In the solid state, the absence of F...F interactions, analyzed by Desiraju⁷ in the structures of fluorinated aromatics, leads to a segregation of the fluorinated and aromatics moieties in –SO₂CF₃-substituted aromatics.⁸

We want to take advantage of this effect, essentially observed in fluid phases, as a structure-orienting tool in

the control of the solid-state architectures of fluorinated molecules, for the rational construction of columnar or layered structures and particularly for the elaboration of conducting or magnetic molecular solids of controlled dimensionality. We also postulate that a limited number of such fluorine atoms, adequately located in the molecular framework, would be sufficient to induce a strong structural effect on the self-assembly properties of those molecules in the solid state.

We describe in this paper the synthesis of the fluorinated 4,5-(2,2'-difluoropropylenedithio)-1,3-dithiole-2-one heterocycle, as a precursor to a variety of different symmetrical and unsymmetrical di- and tetrafluoro-substituted tetrathiafulvalenes with accessible oxidation potentials. The flexibility of the fluorinated seven-membered ring identified from room-temperature NMR data has been thoroughly investigated by temperature-variable ¹H and ¹⁹F NMR experiments, allowing for the identification of two independent folding processes, whose coalescence temperatures (T_c) and activation energies (ΔG^\ddagger) were determined. The analysis of the X-ray crystal structures of three of those fluorinated TTF will demonstrate the efficiency of the nonbonded fluorine exclusion interactions in the control of the solid state arrangement, in addition to S...S van der Waals interactions and C–H...F hydrogen bonds.

Results and Discussion

Syntheses. Several tetrathiafulvalenes bearing fluorinated moieties have been described, as the perfluorodibenzotetrathiafulvalene⁹ or the tetrakis(trifluoromethyl)tetrathiafulvalene,^{10,11} which both exhibit a poor donor ability due to the strong electron-withdrawing

[†] Dedicated to Prof. Fred Wudl on the occasion of his 60th birthday.
(1) Pauling, L. *The Nature of the Chemical Bond*; Cornell University Press: Ithaca, NY, 1960; p 82.

(2) Riess, J. G. *New J. Chem.* **1995**, *19*, 891 and references therein
(3) (a) Höpken, J.; Möller, M. *Macromolecules* **1992**, *25*, 2482. (b) Pensec, S.; Tournilhac, F.-G.; Bassoul P.; Durliat, C. *J. Phys. Chem. B* **1998**, *102*, 52.

(4) Turberg, M. P.; Brady, J. E. *J. Am. Chem. Soc.* **1988**, *110*, 7797.

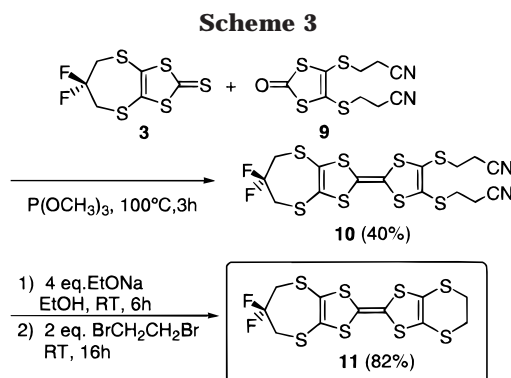
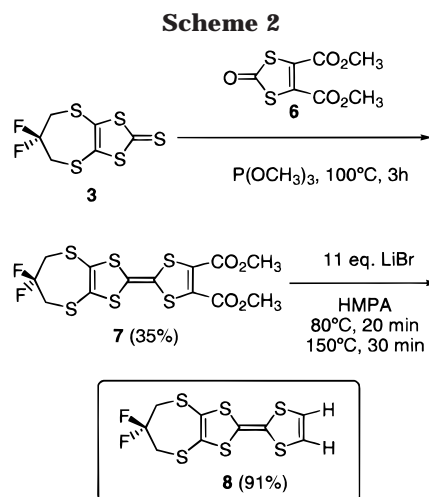
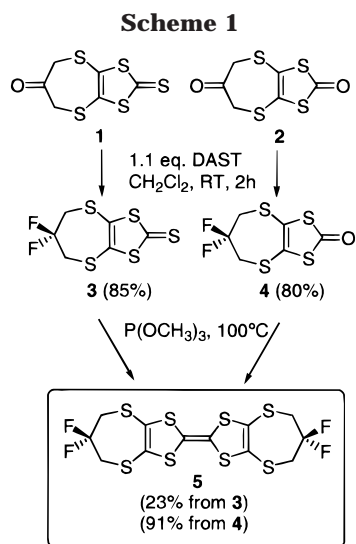
(5) Sadtler, V. M.; Giulieri, F.; Krafft, M.-P.; Riess, J. G. *Chem. Eur. J.* **1998**, *4*, 1952.

(6) (a) Rabolt, J. F.; Russel, T. P.; Twieg, R. J. *Macromolecules* **1984**, *17*, 2786. (b) Russel, T. J.; Rabolt, J. F.; Twieg, R. J.; Siemens, R. L.; Farmer, B. L. *Macromolecules* **1986**, *19*, 1135.

(7) Desiraju, G. R.; Parthasarathy, R. *J. Am. Chem. Soc.* **1989**, *111*, 8725.

(8) Wolff, J.; J. Gredel, F.; Oeser, T.; Irngartinger, H.; Pritzkow, H. *Chem. Eur. J.* **1999**, *5*, 29.

(9) Knight, B. W.; Purrington, S. T.; Bereman, R. D.; Singh, P. *Synthesis* **1994**, 460.



effect of the fluorinated moieties directly conjugated with the TTF. As a consequence, cation radical salts derived from these molecules were never reported. Other examples involve highly soluble TTF cores functionalized with long, flexible C_8F_{17} -perfluoroalkyl chains¹² for the elaboration of Langmuir–Blodgett films.¹³ Looking for alternative substitution patterns that would (i) preserve the donor ability of the π -redox TTF core and (ii) allows for a limited flexibility for good crystallization properties, we envisioned the original tetrathiafulvalene molecules **5**, **8**, and **11**, which meet these requirements. The specificity of these symmetrically or unsymmetrically substituted TTFs lies in the presence of only one or two CF_2 group in a seven-membered ring on one or both sides of the molecule, and isolated from the π -redox active core by the CH_2-S spacers. The key step for the preparation of **5**, **8**, and **11** lies in the successful fluorination of the ketonic group of **1** or **2** by reaction with DAST (Scheme 1).^{14,15} Note the chemoselectivity of this reaction which does not affect the oxygen atom of the dithiocarbonate group in **2**. Indeed, the lowered electrophilicity of the carbonyl group of the dithiocarbonate inhibits the transfer of the nucleophilic fluorine, as also observed with esters.¹⁶ The $P(OMe)_3$ -assisted coupling¹⁷ of the fluorinated dithio- or trithiocarbonate **3** or **4** afforded the symmetrically substituted TTF **5** in 23% yield from **3**, in 91% yield from **4**. The preparation of the unsymmetrically substituted analogues **8** and **11** involves the cross-coupling of the trithiocarbonate **3** with either the diester **6**¹⁸ or with 4,5-bis(2-cyanoethylthio)-1,3-dithiole-2-one **9**.¹⁹ From **3** and **6** (Scheme 2), the fluorinated TTF bearing

one CF_2 group and two ester groups was obtained in good yield after chromatographic separation from the symmetrical coupling products. Decarboxylation²⁰ with LiBr/HMPA occurred in two steps, one CO_2Me group is removed at 80 °C, the second one requires heating to 150 °C, affording the CF_2 -derivatized TTF **8** in excellent yield. Similarly, coupling of **3** with **9**¹⁹ (Scheme 3) afforded the unsymmetrically substituted TTF **10** in good yield. The 2-cyanoethyl moieties in **10** act here as protecting groups for the thiolate groups and can be displaced by action of a strong base such as EtONa. Reaction of the corresponding fluorinated TTF dithiolene with 1,2-dibromoethane afforded the corresponding functionalized TTF **11** in excellent yield. In the course of this work, a second route was also developed for the preparation of the EDT-TTF derivative **11**, which involves the DAST fluorination in the last step for economical reasons given the high price of the DAST reagent (Scheme 4). For that purpose, the ketonic group in **2** was first protected as an acetal **12**. This reaction, described by Marshallsay et al. in 1993,¹⁴ was optimized here by using *p*-toluenesulfonic acid mono hydrate instead of sulfuric acid as acid catalyst. $P(OMe)_3$ -assisted cross coupling of **12** with the dithiocarbonate **13** afforded the acetal-derivatized TTF **14** after chromatographic separation from the symmetrical coupling products. Hydrolysis of **14** regenerated the ketonic group for DAST fluorination of **15**. This last step however proved sluggish despite prolonged gentle heating of the reaction

(10) (a) Hartzler, H. D. *J. Am. Chem. Soc.* **1970**, *92*, 1412; (b) **1973**, *95*, 4379. (c) Bianchini, C.; Meli, A. *J. Chem. Soc., Chem. Commun.* **1983**, 1309. (d) Müller, H.; Lerf, A.; Fritz, H. P. *Liebigs Ann. Chem.* **1991**, 395.

(11) (a) Engler, E. M.; Patel, V. V.; Schumaker, R. R. *J. Chem. Soc., Chem. Commun.* **1979**, 516. (b) Schumaker, R. R.; Engler, E. M. *J. Am. Chem. Soc.* **1980**, *102*, 6652.

(12) Nozdryn, T.; Favard, J.-F.; Cousseau, J.; Jubault, M.; Gorgues, A.; Orduna, J.; Garin, J. *J. Fluorine Chem.* **1997**, *86*, 177.

(13) Dupart, E.; Agricole, B.; Ravaine, S.; Mingotaud, C.; Fichet, O.; Delhaès, P.; Ohnuki, H.; Munger, G.; Leblanc, R. M. *Thin Solid Films* **1994**, *243*, 575.

(14) Marshallsay, G. J.; Bryce, M. R.; Cooke, G.; Jørgensen, T.; Becher, J.; Reynolds, C. D.; Wood, S. *Tetrahedron* **1993**, *49*, 6849.

(15) Middleton, W. J. *J. Org. Chem.* **1975**, *40*, 574.

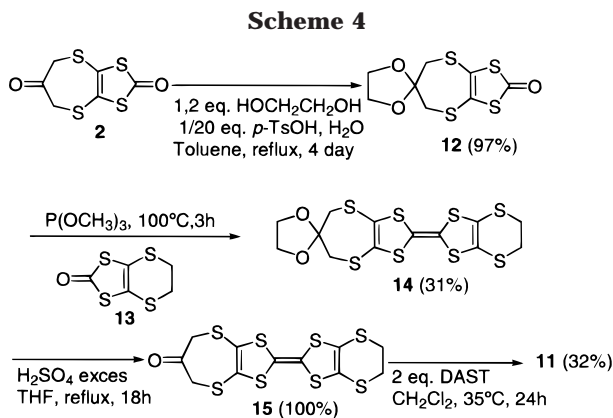
(16) Brunelle, W. H.; McKinnis, B. R.; Narayanan B. A. *J. Org. Chem.* **1990**, *55*, 768.

(17) Reviews: (a) Bryce, M. R. *Aldrichim. Acta* **1985**, *18*, 73. (b) Krief, A. *Tetrahedron* **1986**, *42*, 1209.

(18) Easton, D. B.; Leaver, D. *J. Chem. Soc., Chem. Commun.* **1965**, 22, 585.

(19) Sventrup, N.; Rasmussen, K. M.; Hansen, T. K.; Becher, J. *Synthesis* **1994**, 8, 809.

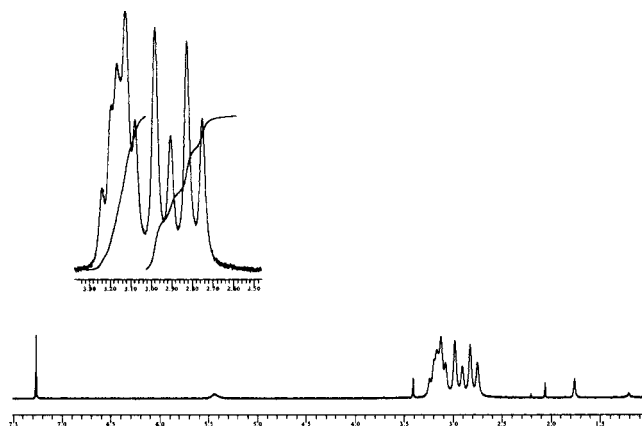
(20) Lakshmikantham, M. V.; Cava, M. P. *J. Org. Chem.* **1976**, *41*, 882.



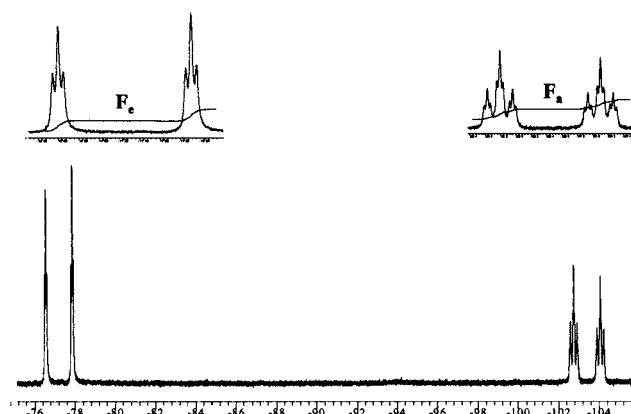
mixture and only 32% of the desired TTF was obtained by this route.

Two Independent Folding Processes Identified by Variable-Temperature ^1H and ^{19}F NMR Studies. The fluorine atoms of all these fluorinated molecules were not observed by ^{19}F NMR at room temperature where only very broad nearly indistinguishable massifs were obtained. The fluxional behavior of the seven-membered ring incorporating the difluoromethylene moiety was confirmed by low-temperature ($-30\text{ }^\circ\text{C}$) NMR experiments that allowed for the observation of the ^{19}F NMR spectra. Under those conditions, however, most of the molecules described here precipitated in the NMR tubes. Therefore, a complete NMR study of this fluxional behavior has been performed only on the most soluble compound (**4**), in CDCl_3 at low temperatures ($\leq 10\text{ }^\circ\text{C}$) and in C_6D_6 at higher temperatures ($\geq 10\text{ }^\circ\text{C}$).

As shown in Figure 1a, the ^1H NMR spectrum of **4** shows two multiplets at δ 2.75 and 3.15 suggesting the presence of two types of hydrogen nuclei (2H_a and 2H_e). In the same way, the ^{19}F NMR spectrum (Figure 1b) shows two doublets of triplets of triplets at δ -77 and -103.5 suggesting the presence of two different fluorine atoms (F_e and F_a). We can reasonably consider that, at this temperature, the dithiocarbonate **4** is in its most stable configuration, that is to say a chair form (Figure 2). The attribution of the different signals was based on the fluorine atom F_a , which is expected to be shielded by the lone pairs of the neighboring sulfur atom. So its signal was considered to be at -103 ppm . This hypothesis was supported by the analysis of its heteronuclear coupling constants ($^3J_{\text{FH}}$) considering the Karplus²¹ rules that link the 3J coupling constants with the dihedral angle (Φ). According to those rules, J_{cis} ($\Phi = 60^\circ$) should be less than J_{trans} ($\Phi = 180^\circ$). So we expect here J_{FaHa} to be larger than J_{FaHe} , J_{FeHa} , and J_{FeHe} . The signal attributed to F_a (δ -103.5) follows these rules with a doublet ($^2J_{\text{FaFe}} = 247\text{ Hz}$) of triplets ($^3J_{\text{FaHa}} = 31\text{ Hz}$) of triplets ($^3J_{\text{FaHe}} = 7\text{ Hz}$) with indeed $^3J_{\text{FaHe}} < ^3J_{\text{FaHa}}$. The ^{19}F signal positioned at lower field (δ -77) is attributed to F_e with a doublet ($^2J_{\text{FeFa}} = 247\text{ Hz}$) of triplets ($^3J_{\text{FeHe}} = 10\text{ Hz}$) while $^3J_{\text{FeHa}}$ is probably too small to be seen. A similar analysis performed on the ^1H NMR spectrum drives us to conclude that the signal located at δ 2.75 must be attributed at the two axial protons H_a with the large $^3J_{\text{HF}}$ coupling constant ($^3J_{\text{FaHa}} = 31\text{ Hz}$) observed in this multiplet while the signal located at δ 3.15 must be attributed to the two equatorial protons H_e with smaller $^3J_{\text{HF}}$ coupling constants.



(a)



(b)

Figure 1. ^1H (a) and ^{19}F (b) NMR spectra of compound **4** in CDCl_3 at $-30\text{ }^\circ\text{C}$.

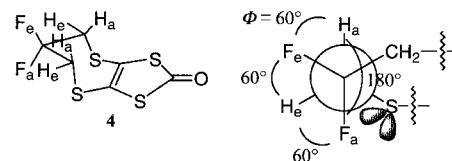


Figure 2. Left: the most stable conformation of **4**. Right: a Newman representation of **4** with the dihedral angles between the different nuclei F_a , F_e , H_a , and H_e (a and e stand for axial and equatorial, respectively).

The variable-temperature ^1H and ^{19}F NMR studies showed two independent folding processes. The first one is observed at low temperature ($T_c = -15\text{ }^\circ\text{C}$) on the ^1H NMR spectra (Figure 3) where the two massifs attributed to H_e and H_a coalesce upon warming from $-30\text{ }^\circ\text{C}$, while in the ^{19}F spectra (Figure 4), a broadening of the peaks reflects the equivalence of the two types of hydrogen nuclei. This low-temperature folding process can therefore be attributed to an inversion around the $\text{C}3\text{--C}5$ axis (Figure 5). The activation energy for this fluxional behavior is estimated at 50.2 kJ mol^{-1} from the Eyring equation.²² The second process, which occurs at higher temperature, is observed on the ^{19}F NMR spectra (Figure 4). Both broad room-temperature singlets attributed to F_a and F_e coalesce upon warming in a broad singlet above

(21) Karplus, M. *J. Am. Chem. Soc.* **1963**, *85*, 2870.

(22) Eyring, H. *Chem. Rev.* **1935**, *17*, 65.

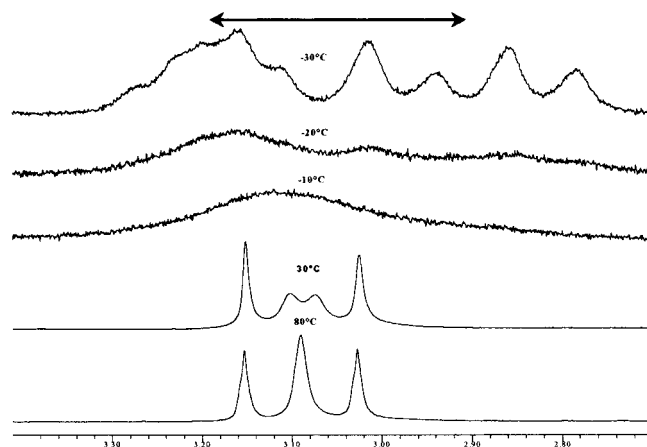


Figure 3. Variable-temperature ^1H NMR for compound **4** in CDCl_3 .

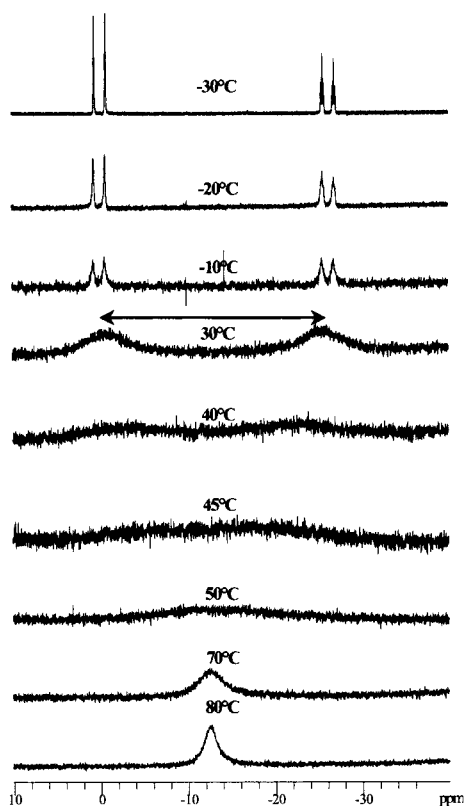


Figure 4. Variable-temperature ^{19}F NMR for compound **4** in C_6D_6 .

$T_c = 47^\circ\text{C}$ ($\Delta G^\ddagger = 51.1\text{ kJ mol}^{-1}$) where the two fluorine nuclei become magnetically undistinguishable. As a consequence, the ^1H NMR spectra (Figure 3) change from an ABX_4 system at room temperature to an A_2X_4 one above 47°C . This second process corresponds to an inversion around the S1-S4 axis (Figure 5).

Fluorine Segregation Controls the Structures of the Neutral Donor Molecules. The symmetrically substituted tetrathiafulvalene **5** crystallizes as thin red plates from toluene in the monoclinic system, space group $P2_1/c$. As shown in Figure 6, a full segregation of the heteroaromatic and the fluorinated moieties is observed, giving rise to a unique layered structure with stacks of molecules and a compact fluorinated bilayer: the first-neighbor $\text{F}\cdots\text{F}$ distances vary between $2.769(3)$ and $3.254(3)$ Å, values around the van der Waals $\text{F}\cdots\text{F}$

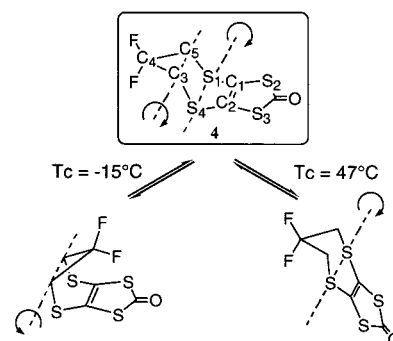


Figure 5. The two folding processes observed in **4**.

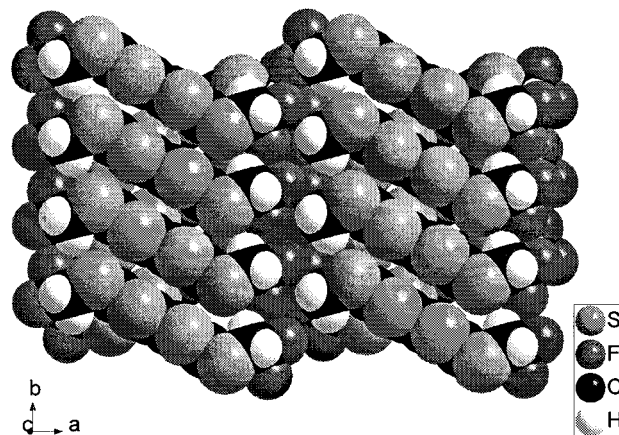


Figure 6. View of the layered structure of **5** along the c axis showing the fluorine segregation.

Table 1. Geometrical Characteristics of the $\text{CH}\cdots\text{F}$ Hydrogen Bonds in **5, **8**, and **11****

compd	interaction	$\text{H}\cdots\text{F}$ (Å)	$\text{C}\cdots\text{F}$ (Å)	$\text{C-H}\cdots\text{F}$ ($^\circ$)
5	$\text{C4H4A}\cdots\text{F12}$	2.958	3.794	144.9
	$\text{C4H4A}\cdots\text{F22}$	2.702	3.512	141.4
	$\text{C4H4B}\cdots\text{F13}$	2.741	3.412	126.8
	$\text{C6H6A}\cdots\text{F13}$	2.612	3.304	128.5
	$\text{C6H6B}\cdots\text{F12}$	2.491	3.408	157.5
	$\text{C6H6B}\cdots\text{F22}$	2.692	3.473	137.8
8	$\text{C}_{\text{sp}2}\text{1H1}\cdots\text{F22}$	2.542	3.314	140.6
	$\text{C}_{\text{sp}2}\text{2H2}\cdots\text{F12}$	2.800	3.653	152.8
	$\text{C9H9B}\cdots\text{F12}$	2.759	3.459	129.6
11	$\text{C4H4B}\cdots\text{F12}$	2.362	3.145	137.3
	$\text{C9H9B}\cdots\text{F22}$	2.529	3.221	128.3
	$\text{C10H10B}\cdots\text{F22}$	2.691	3.553	148.3
	$\text{C10H10A}\cdots\text{F22}$	2.779	3.211	107.7

distance (2.94 Å).²³ This arrangement results from the interplay between (i) the $\text{S}\cdots\text{S}$ van der Waals interactions which stabilize the face-to-face stacking of the TTF cores along the b axis and the lateral arrangement of these stacks along the c direction and (ii) the striking full segregation of the CF_2 groups on the outer ends of these layers. In addition, short $\text{C-H}\cdots\text{F}$ distances within a layer and through the $\text{F}\cdots\text{F}$ van der Waals gap are also observed (Table 1), with geometrical features comparable to those reported by Desiraju²⁴ in *p*-difluorobenzene ($d_{\text{H}\cdots\text{F}} = 2.49$ Å).²⁵ These $\text{C-H}\cdots\text{Hal}$ hydrogen bonds,²⁶ albeit weak in essence, have been shown to play a crucial role in the organic solid state of halogenated molecules, and despite the fact that the fluorine atoms are poor hydrogen

(23) Bondi, A. *J. Phys. Chem.* **1964**, *68*, 441.

(24) Thalladi, V. R.; Weiss, H.-C.; Bläser, D.; Boese, R.; Nangia, A.; Desiraju, G. R. *J. Am. Chem. Soc.* **1998**, *120*, 8702.

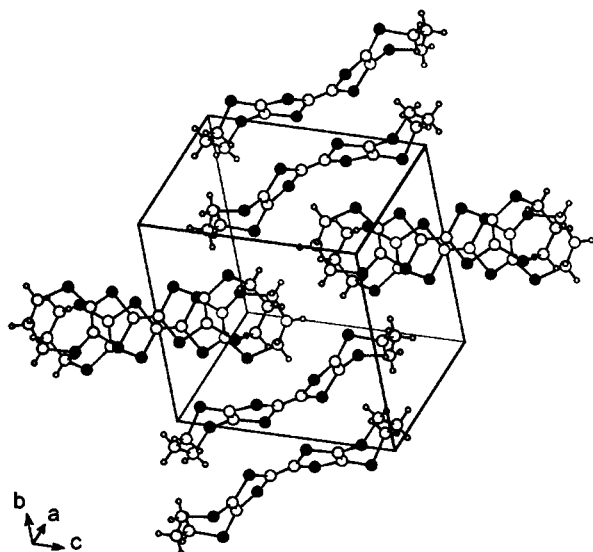


Figure 7. View of the unit cell of the nonfluorinated analogue of **5**, the bis(propylenedithio)tetrathiafulvalene with the usual orthogonal inversion-centered dimers.

bond acceptors, the hydrogen bond donor character of the methylenic moieties in **5** is most probably enhanced here by the presence of the neighboring electron-withdrawing CF_2 entities. An enlightening comparison can be made with the structure of the nonfluorinated analogue, the bis(propylenedithio)tetrathiafulvalene (BPDT-TTF), which crystallizes into orthogonal inversion-centered dimers (Figure 7),²⁷ as most frequently observed with those sulfur-rich molecules such as EDT-TTF²⁸ or BEDT-TTF,²⁹ whose structures are mainly controlled by $\text{S}\cdots\text{S}$ van der Waals interactions. On the other hand, in the structure of the tetrakis(trifluoromethyl)tetrathiafulvalene,³⁰ the criss-cross arrangement of the molecules on top of each other gives rise to cylindrical stacks with all CF_3 groups exposed to the surface through similar fluorine segregation effects. These columns then organize into a pseudo-hexagonal array reminiscent of thermotropic discotic phases. Thus in **5**, the outer difluoromethylene groups are responsible for inducing an original layered solid state arrangement which is not usually observed with those molecules in their neutral, unoxidized state. Also this structure is reminiscent of that observed in smectic liquid crystalline phases. DSC measurements were performed with **5** in an attempt to observe such a behavior but only decomposition, at 306 °C, was observed upon heating.

The X-ray structures of the unsymmetrically substituted fluorinated TTF **8** and **11** confirm those trends

(25) Such C–H \cdots F interactions were also recently reported in the bis(ethylenedithio)tetrathiafulvalene (BEDT-TTF) salt of 2-fluorotetracyanoquinodimethane (F₁TCNQ): Hasegawa, T.; Inukai, K.; Kagoshima, S.; Sugawara, T.; Mochida, T.; Sugiura, S.; Iwasa, Y. *J. Chem. Soc. Chem. Commun.* **1997**, 1377.

(26) Desiraju, G. R.; Steiner, T. In *The Weak Hydrogen Bond*; Oxford University Press: New York, 1999.

(27) Porter, L. C.; Kini, A. M.; Williams, J. M. *Acta Crystallogr. C* **1987**, *43*, 998.

(28) Garreau, B.; De Montauzon, D.; Cassoux, P.; Legros, J.-P.; Fabre, J.-M.; Saoud, K. Chakroune, S. *New J. Chem.* **1995**, *19*, 161.

(29) (a) Kobayashi, H.; Kato, R.; Mori, T.; Ayashi, A.; Saki, Y.; Saito, G.; Inokuchi, H. *Chem. Lett.* **1983**, 759. (b) Kobayashi, H.; Kato, R.; Kobayashi, A.; Mori, T.; Inokuchi, H. *Solid State Commun.* **1986**, *40*, 473.

(30) Mono, S.; Pritzkow, H.; Sundermeyer, W. *Chem. Ber.* **1993**, *126*, 2111.

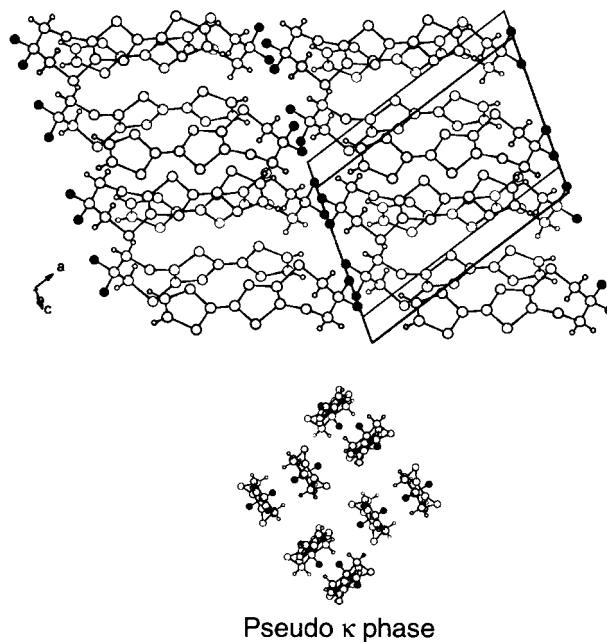


Figure 8. Top: a view of the unit cell of **8**, showing the fluorine (in black) segregation and the layered structure. Bottom: detail of one organic slab, viewed along the long molecular axis of **8**.

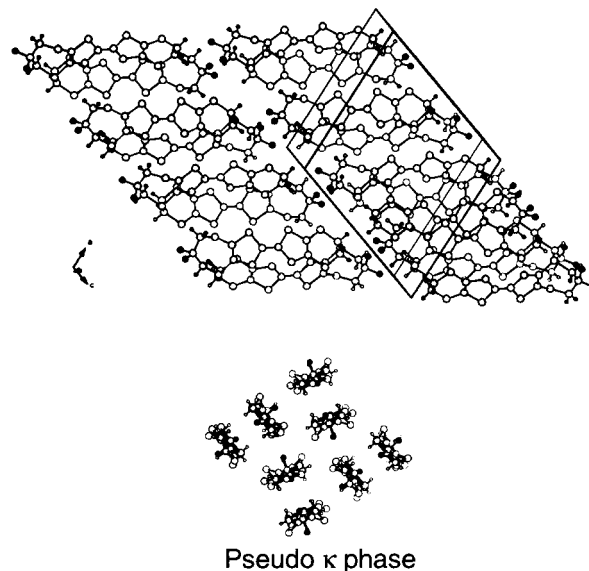
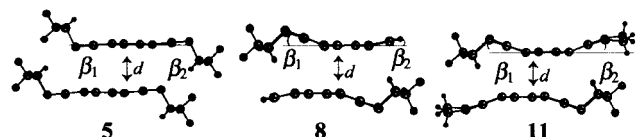


Figure 9. Top: a view of the unit cell of **11**, showing the fluorine (in black) segregation and the layered structure. Bottom: detail of one organic slab, viewed along the long molecular axis of **11**.

despite the presence of only one CF_2 group. As shown in Figures 8 and 9, the donor molecules crystallize into inversion-related face-to-face dimers, with an interplanar distance of 3.557(3) and 3.443(1) Å in **8** and **11**, respectively (Table 2). Note that the molecules are strongly distorted from planarity; the dithiole rings of the central TTF core are indeed folded along the S–S axis by 21.29(6) and 12.0(1)° in **8**, 20.18(5) and 19.20(5)° in **11**. Those diads then organize in the solid state in a layered motif characterized by the same fluorine segregation observed with **5** and the presence of C–H \cdots F hydrogen bonds (Table 1) which involve not only the methylenic groups ($-\text{SCH}_2\text{CF}_2-$) of **8** and **11** but also the ethylenic hydrogen

Table 2. Interplanar Distances and Folding Angles for **5**, **8**, and **11**

compd	torsion angle β_1 (deg)	torsion angle β_2 (deg)	distance d (Å)
5	7.6(3)	7.6(3)	4.094(8)
8	21.29(6)	12.0(1)	3.557(3)
11	20.18(5)	19.20(5)	3.443(1)

Table 3. Oxidation Potentials of **5**, **8**, and **11**

compd	solvent	$E^{1/2^a}$	$E^{2/2^a}$
5	THF	0.87	1.07
BPDT-TTF	THF	0.74	0.92
8	CH ₃ CN	0.48	0.82
EDT-TTF	CH ₃ CN	0.44	0.75
11	CH ₃ CN	0.58	0.83
BEDT-TTF	CH ₃ CN	0.56	0.80
BPDT-TTF	CH ₃ CN	0.54	0.81

^a In V vs SCE; supporting electrolyte, 0.1 M Bu₄NPF₆, scan rate, 0.1 V s⁻¹.

atoms of **8**. Note that the organization of the molecular dimers within the slabs is reminiscent of the so-called κ phases of conducting and superconducting BEDT-TTF salts. This rare κ -phase organization in the structure of *neutral* donor molecules,³¹ characterized by the mean planes of contacting molecules being almost perpendicular and their principal axes essentially parallel, is all the more fortunate since it might be conserved in the cation radical salts of those fluorinated donor molecules.

Electrochemical Properties. Cyclic voltammetry data for the new donor molecules are collected in Table 3 together with those of reference compounds TTF, BEDT-TTF, and BPDT-TTF. They all exhibit two reversible oxidation waves, as expected for TTF derivatives. The comparison of the first oxidation potential of **5**, observed at 0.87 V vs SCE in THF,³² with its nonfluorinated analogue the bis(propylenedithio)tetrathiafulvalene (BPDT-TTF) (0.74 V vs SCE in THF) shows that the four fluorine atoms exert a small but noticeable anodic shift despite the CH₂-S spacers of the seven-membered rings. The same effect is observed to a less extent in **8** and **11**, when compared with the non fluorinated EDT-TTF or BEDT-TTF analogues. Those values are also to be compared with those of (CF₃)₄-TTF^{10,11} or perfluorodibenzotetrathiafulvalene⁹ which oxidize at much higher potentials in CH₃CN, 1.05 and 1.45 V vs SCE, respectively, demonstrating the soundness of our approach. Accordingly, **5** could be successfully electrocrystallized in the presence of various electrolytes such as the *n*-Bu₄N⁺ salts of the linear anions ICl₂⁻, IBr₂⁻, and I₂Br⁻, affording, air-stable crystalline salts whose structures and magnetic properties will be described elsewhere.

(31) One other example has been described: Batsanov, A. S.; Bryce, M. R.; Cooke, G.; Dhindsa, A. S.; Heaton, J. N.; Howard, J. A. K.; Moore, A. J.; Petty, M. C. *Chem. Mater.* **1994**, *6*, 1419.

(32) The use of THF, for solubility reasons, in the characterization of **5** introduces an extra anodic shift when compared with measurements performed in CH₃CN. See also: Lichtenberger, D. L.; Johnston, R. L.; Hinkelmann, K.; Suzuki, T.; Wudl, F. *J. Am. Chem. Soc.* **1990**, *112*, 3302.

Conclusion

This work provides an easy access to a novel class of symmetrically as well as asymmetrically substituted fluorinated TTFs where the CF₂ groups are not conjugated with the TTF π redox core, as confirmed by the accessible oxidation potentials. The intermolecular F \cdots F nonbonded interactions observed in the solid state, combined with C-H \cdots F hydrogen bonds, afford layered structures, an highly unusual organization motif for TTF molecules in their *neutral* state.

Experimental Section

General Considerations. Unless otherwise indicated, all reactions were carried out under nitrogen. Solvents (dichloromethane, acetonitrile) were dried and freshly distilled over P₂O₅. Note that DAST and related dialkylaminosulfur trifluorides should not be heated since they are said to undergo catastrophic decomposition (explosion or detonation) with gas evolution upon heating above 90 °C.³³ ¹H, ¹³C, and ¹⁹F NMR spectra were recorded at 200 (¹H, ¹⁹F) and 50 MHz (¹³C). The chemical shifts are given in δ ppm, downfield from internal Me₄Si for ¹H and ¹³C NMR, upfield from external CFCl₃ for ¹⁹F NMR. Mass spectra were taken in the EI mode with an ionization energy of 70 eV and a current intensity of 300 μ A. Cyclic voltammetry were taken with a Pt disk (ϕ = 1 mm) as working electrode and a Pt wire as counter electrode and a SCE as reference electrode. Elemental analyses were performed either at the Service Central d'Analyse (CNRS), Vernaison, France or the Institut de Chimie des Substances Naturelles (CNRS), Gif/Yvette, France.

6,6-Difluoro-5,7-dihydro-5H-[1,3]dithiolo[4,5-*b*][1,4]-dithiepin-2-thione (3**).** **1** (2 g, 7.94 mmol) was dissolved in dry CH₂Cl₂ (200 mL). A solution of DAST (1.16 mL, 8.7 mmol) in CH₂Cl₂ (4 mL) was added dropwise at 0 °C, and the mixture was allowed to warm to room temperature and stirred for 2 h. The reaction mixture was poured into ice-cold water (200 mL), the lower organic layer was separated, washed with water, and dried (MgSO₄), and the solvent was evaporated to afford 2.1 g of crude product, which was purified by column chromatography (silica gel, dichloromethane) and recrystallization from acetonitrile to give orange needles of **3** (1.85 g, 85%): mp 192 °C (CH₃CN); R_f = 0.85 (CH₂Cl₂); IR (KBr) 1078, 1039 cm⁻¹; ¹H NMR (CDCl₃, 200 MHz) δ 2.99 (4H, m); ¹³C NMR (CDCl₃, 50 MHz) δ 38.13 (2C, t, J = 30 Hz), 121.04 (2C, t, J = 239 Hz), 137.80, 209.20; EIMS (m/z) 274 (M⁺, 77), 198 (37), 88 (100). Anal. Calcd for C₆H₄F₂S₅ (274.425): C, 26.26; H, 1.47; F, 13.85; S, 58.42. Found: C, 26.31; H, 1.37; F, 13.51; S, 58.38.

6,6-Difluoro-5,7-dihydro-5H-[1,3]dithiolo[4,5-*b*][1,4]-dithiepin-2-one (4**).** This compound (3.5 g, 80%) was prepared from **2** (4 g, 16.9 mmol) and DAST (2.48 mL, 18.6 mmol) as a white solid, employing the same procedure as described above for compound **3**. Recrystallization from acetonitrile afforded **4** as gray needles: mp 183 °C (CH₃CN); R_f = 0.80 (CH₂Cl₂); IR (KBr) 1664, 1080 cm⁻¹; ¹H NMR (CDCl₃, 200 MHz) δ 3.03 (4H, m); ¹³C NMR (CDCl₃, 50 MHz) δ 38.35 (2C, t, J = 29 Hz), 120.91 (2C, t, J = 244 Hz), 131.26, 188.02; EIMS (m/z) 258 (M⁺, 93), 230 (51), 154 (51), 88 (100). Anal. Calcd for C₆H₄F₂O₁S₄ (258.358): C, 27.89; H, 1.56; F, 14.71; S, 49.65. Found: C, 27.93; H, 1.52; F, 14.28; S, 49.91.

Bis(difluoropropylenedithio)tetrathiafulvalene (5**).** **From 3.** A mixture of **3** (0.1 g, 0.365 mmol) and freshly distilled P(OMe)₃ (60 equiv) was refluxed for 1 h. The reaction mixture was allowed to cool to room temperature and an equal volume of methanol was added. The precipitate was filtered and washed with ethanol and diethyl ether to give the crude product as a red powder. Two recrystallizations from toluene afforded red plates of **5** (20 mg, 23%)

(33) Messina, P. A.; Mange, K. C.; Middleton, W. J. *J. Fluorine Chem.* **1989**, *42*, 137.

From 4. A mixture of **4** (0.4 g, 1.55 mmol) and freshly distilled P(OMe)₃ (60 equiv) was refluxed for 3 h. The reaction mixture was allowed to cool to room temperature, and an equal volume of methanol was added. The precipitate was filtered and washed with ethanol and diethyl ether to give the crude product as a red powder. Two recrystallizations from toluene afforded red plates of **5** (300 mg, 80%): mp 306 °C (toluene, dec); $R_f = 0.85$ (CH₂Cl₂); IR (KBr) 1075 cm⁻¹; ¹H NMR (DMSO/CS₂, 200 MHz) δ 3.03 (8H, m); EIMS (m/z) 484 (M⁺, 83), 286 (38), 198 (42), 88 (100). Anal. Calcd for C₁₂H₈F₄S₈ (484.717): C, 29.74; H, 1.66; F, 15.68; S, 52.92. Found: C, 30.01; H, 1.64; F, 15.04; S, 52.74.

2-[1,3]Dithiol-2-ylidene-6,6-difluoro-5,7-dihydro-5H-[1,3]dithiolo[1,4]dithiepin-4,5-dicarboxylic Acid Dimethyl Ester (7). A mixture of **3** (2 g, 7.3 mmol) and the diester **6** (1.71 g, 7.3 mmol) in freshly distilled P(OMe)₃ (120 mL) was refluxed for 3 h. The reaction mixture was allowed to cool to room temperature. The precipitate was filtered, washed with ethanol and diethyl ether to give 0.59 g of F₄BPDT-TTF **5** (20%) as a red microcrystalline powder. Concentration of the filtrate followed by column chromatography (silica gel, toluene) afforded 1.25 g of the diester **7**. The resulting dark red solid can be further purified by recrystallization from toluene/cyclohexane (3/7) to give **7** (1.18 g, 35%) as dark red needles: mp 224 °C (toluene/cyclohexane 3:7); R_f = 0.49 (toluene); IR (KBr) 1721, 1250, 1020 cm⁻¹; ¹H NMR (CDCl₃, 200 MHz) δ 2.95 (4H, m), 3.84 (6H, s); EIMS (m/z) 460 (M⁺, 37), 198 (38), 88 (100). Anal. Calcd for C₁₃H₁₀F₂O₄S₆ (460.613): C, 33.90; H, 2.19; F, 8.25; S, 41.77. Found: C, 34.06; H, 2.21; F, 7.92; S, 42.02.

2-[1,3]Dithiol-2-ylidene-6,6-difluoro-5,7-dihydro-5H-[1,3]dithiolo[4,5-*b*][1,4]dithiepine (8). A suspension of lithium bromide (1.09 g, 11 equiv, 12.5 mmol) in hexamethylphosphoric triamide (30 mL) was stirred at 80 °C (LiBr dissolved at 60 °C). The diester **7** (500 mg, 1.09 mmol) was added, and the mixture was stirred for a further 20 min (the first decarboxylation occurred). The second decarboxylation was obtained by increasing the temperature to 150 °C and stirring the solution for 30 min. After being cooled at room temperature, the reaction mixture was diluted with ethyl acetate (250 mL), washed with brine (3 × 150 mL), dried over MgSO₄, and concentrated. The residue was subjected to column chromatography with toluene (degassed with N₂) as eluent. One recrystallization from acetonitrile afforded **8** as red crystals (340 mg, 91%): mp 191 °C (CH₃CN); $R_f = 0.9$ (toluene); IR (KBr) 1411, 1253, 1067 cm⁻¹; ¹H NMR (CDCl₃, 200 MHz) δ 2.94 (4H, m), 6.34 (2H, s); ¹³C NMR (CDCl₃, 50 MHz) δ 38.35 (2C, t, $J = 29$ Hz), 105.50, 120.91 (2C, t, $J = 244$ Hz), 131.77; EIMS (m/z) 344 (M⁺, 100), 146 (88), 102 (49), 88 (57). Anal. Calcd for C₉H₆F₂S₆ (344.539): C, 31.37; H, 1.76; F, 11.03; S, 55.84. Found: C, 31.51; H, 2.21; F, 10.83; S, 55.69.

2,3-Bis(2-cyanoethylthio)-5,7-(6,6-difluoropropylene-dithio)tetrathiafulvalene (10). A mixture of **3** (2 g, 7.3 mmol) and 4,5-bis(2-cyanoethylthio)-1,3-dithiole-2-one **9**¹⁹ (2 g, 7.3 mmol) in P(OMe)₃ (100 mL, freshly distilled) was refluxed for 6 h. The reaction mixture was allowed to cool to room temperature. The precipitate was filtered and washed with ethanol and diethyl ether to give 0.40 g of **5** (15%) as a red microcrystalline powder. Concentration of the filtrate followed by column chromatography (silica gel, CH₂Cl₂) afforded 1.6 g (43%) of the bis-cyanoethyl protected TTF **10**. The resulting yellow solid can be further purified by recrystallization from acetonitrile to give 1.5 g (40%) of yellow platelets of **10**: mp 191 °C (CH₃CN); $R_f = 0.29$ (CH₂Cl₂); IR (KBr) 2977, 2920, 2250, 1260, 1077 cm⁻¹; ¹H NMR (CDCl₃, 200 MHz) δ 2.74 (t, 2H, $J = 6.8$ Hz), 2.95 (4H, m), 3.09 (t, 2H, $J = 6.8$ Hz); EIMS (m/z) 514 (M⁺, 51), 286 (100), 166 (67), 88 (89). Anal. Calcd for C₁₅H₁₂F₂N₂S₈ (514.799): C, 35.00; H, 2.35; F, 7.38; N, 5.44; S, 49.83. Found: C, 35.06; H, 2.31; F, 6.76; N, 5.21; S, 50.13.

2,3-(Ethylenedithio)-5,7-(6,6-difluoropropylene-dithio)tetrathiafulvalene (11). From TTF **10**. A solution of sodium methanolate (previously prepared from sodium (36 mg, 1.56 mmol, 4 equiv) in MeOH (3 mL) was added dropwise to a suspension of **10** (200 mg, 0.39 mmol) in degassed MeOH (25

mL) at room temperature. After being stirred for 6 h, the red limpid solution was treated with 2 equiv of 1,2-dibromoethane (69 μ L, 0.8 mmol) and the reaction mixture stirred for 12 h. The precipitation of **11** was completed by cooling the reaction mixture at 0 °C. The precipitate was filtered and washed with cold EtOH (20 mL) and cold Et₂O (20 mL). Purification by column chromatography (silica gel, CH₂Cl₂/cyclohexane) followed by recrystallization from toluene give 140 mg (82%) of orange platelets of **11**.

From 15. The TTF **15** (90 mg, 0.218 mmol) was dissolved in dry CH₂Cl₂ (150 mL) and cooled to 0 °C. A solution of DAST (32 μ L, 0.243 mmol) in CH₂Cl₂ (2 mL) was added dropwise, and the mixture was carefully warmed to 35 °C and stirred for 24 h. The reaction mixture was poured into ice-cold water (150 mL), the lower organic layer was decanted, washed with water, and dried (MgSO₄), and the solvent was evaporated to afford 50 mg of crude product, which was purified by column chromatography (silica gel, toluene) and recrystallization from toluene to give orange platelets of **11** (30 mg, 32%): mp 226 °C (toluene); $R_f = 0.58$ (CH₂Cl₂/cyclohexane); IR (KBr) 1262, 1076 cm⁻¹; ¹H NMR (CDCl₃, 200 MHz) δ 2.93 (4H, m), 3.29 (4H, s); EIMS (m/z) 434 (M⁺, 72), 406 (39), 166 (53), 88 (100). Anal. Calcd for C₁₁H₈F₂S₈ (434.709): C, 30.39; H, 1.85; F, 8.74; S, 59.01. Found: C, 30.51; H, 1.83; F, 8.50; S, 58.07.

Ketal-Protected [1,3]Dithiolo[4,5-*b*][1,4]dithiepine-2,6-dione (12). To a solution of **2** (4 g, 16.9 mmol) in dry toluene (50 mL) were added ethylene glycol (1.14 mL, 20.34 mmol) and TsOH·H₂O (0.161 g, 0.85 mmol). A Dean–Stark apparatus was assembled and the reaction refluxed with stirring for 4 days. The organic phase was washed with a solution of sodium hydrogen carbonate (2 × 200 mL), dried (MgSO₄), and concentrated. The crude product was recrystallized from acetonitrile to afford white needles of **12** (4.57 g, 97%): mp 145 °C (CH₃CN); $R_f = 0.59$ (CH₂Cl₂); IR (KBr) 2993, 2896, 1660, 1610 cm⁻¹; ¹H NMR (CDCl₃, 200 MHz) δ 2.83 (4H, s), 4.09 (4H, s); EIMS (m/z) 280 (M⁺, 40), 194 (100), 166 (47). Anal. Calcd for C₈H₆O₃S₄ (280.414): C, 34.27; H, 2.88; O, 17.12; S, 45.74. Found: C, 34.23; H, 2.91; O, 17.36; S, 45.71.

Ketal-Protected 2,3-(Ethylenedithio)-5,7-(6-oxopropylene-dithio)tetrathiafulvalene (14). A mixture of the ketal **12** (1 g, 3.60 mmol) and 4,5-ethylenedithio-1,3-dithiol-2-one **13** (750 mg, 3.60 mmol) in P(OMe)₃ (12.5 mL, freshly distilled) was refluxed for 6 h. The reaction mixture was allowed to cool to room temperature. Concentration of the solution followed by column chromatography (silica gel, toluene) and recrystallization from toluene afforded 510 mg (31%) of brown needles of the ketal protected TTF **14**: mp 248 °C (toluene); $R_f = 0.36$ (toluene); IR (KBr) 2960, 2911, 1100, 1000 cm⁻¹; ¹H NMR (CDCl₃, 200 MHz) δ 2.72 (4H, s), 3.28 (s, 4H), 4.09 (4H, s); EIMS (m/z) 456 (M⁺, 100), 428 (63), 264 (90). Anal. Calcd for C₁₃H₁₂O₂S₈ (456.765): C, 34.18; H, 2.65; O, 7.01; S, 56.16. Found: C, 34.46; H, 2.72; O, 7.26; S, 54.51.

2,3-(Ethylenedithio)-5,7-(6-oxopropylene-dithio)tetrathiafulvalene (15). A solution of ketal-protected TTF **14** (200 mg, 0.438 mmol) in THF (100 mL) was acidified with concentrated sulfuric acid (10 mL) and the mixture refluxed for 18 h. After being cooled at room temperature, the solution was concentrated, taken up in CH₂Cl₂ (100 mL), washed with brine (2 × 100 mL), dried (MgSO₄), and concentrated. The crude product was purified by column chromatography (silica gel, CH₂Cl₂) and recrystallization from toluene to give yellow platelets of **15** (180 mg, 100%): mp 227 °C (toluene); $R_f = 0.60$ (toluene); IR (KBr) 2964, 2916, 1704 cm⁻¹; ¹H NMR (CDCl₃, 200 MHz) δ 3.29 (4H, s), 3.35 (4H, s); EIMS (m/z) 412 (M⁺, 87), 88 (100). Anal. Calcd for C₁₁H₈OS₈ (412.713): C, 32.01; H, 1.95; O, 3.88; S, 62.16. Found: C, 31.97; H, 1.97; O, 4.66; S, 61.09.

X-ray Crystallography. The X-ray measurements were carried out on crystals mounted on glass fibers using a Stoe IPDS (for **5**) or an Enraf-Nonius Mach3 diffractometer (for **8** and **11**) with graphite-monochromated Mo K α radiation ($\lambda = 0.71069$ Å) at 293 K. A numerical absorption correction was applied for **5** and none for **8** and **11**. The structures were solved by direct methods (SHELXS) and refined by full-matrix least-squares (SHELXL). The hydrogen atoms were included at

idealized positions ($d(\text{C}-\text{H}) = 0.97 \text{ \AA}$ in sp^3 methylenic hydrogen atoms and $d(\text{C}-\text{H}) = 0.93 \text{ \AA}$ in $\text{sp}^2 = \text{CH}$ aromatic hydrogen atoms) and not refined. Data for **5**: $\text{C}_{12}\text{H}_8\text{F}_4\text{S}_8$, MW = 484.66, red plate, monoclinic, $P2_1/c$, $a = 15.460(2) \text{ \AA}$, $b = 4.5991(5) \text{ \AA}$, $c = 13.0492(13) \text{ \AA}$, $\beta = 109.201(13)^\circ$, $V = 876.2(2) \text{ \AA}^3$, $Z = 2$, $D_{\text{calc}} = 1.837 \text{ g cm}^{-3}$, $\mu = 1.051 \text{ mm}^{-1}$, $R(\text{F}) = 0.035$, $wR(\text{F}^2) = 0.0564$. Data for **8**: $\text{C}_9\text{H}_6\text{S}_2\text{S}_6$, MW = 344.50, red plate, monoclinic, $P2_1/c$, $a = 13.649(3) \text{ \AA}$, $b = 10.996(2) \text{ \AA}$, $c = 9.1740(18) \text{ \AA}$, $\beta = 118.44(3)^\circ$, $V = 1306.2(4) \text{ \AA}^3$, $Z = 4$, $D_{\text{calc}} = 1.752 \text{ g cm}^{-3}$, $\mu = 1.042 \text{ mm}^{-1}$, $R(\text{F}) = 0.0345$, $wR(\text{F}^2) = 0.0794$. Data for **11**: $\text{C}_{11}\text{H}_8\text{F}_2\text{S}_8$, MW = 434.65, red plate, monoclinic, $P2_1/c$, $a = 13.598(1) \text{ \AA}$, $b = 8.869(1) \text{ \AA}$, $c = 14.303(1) \text{ \AA}$, $\beta = 107.93(1)^\circ$, $V = 1641.2(2) \text{ \AA}^3$, $Z = 4$, $D_{\text{calc}} = 1.759 \text{ g cm}^{-3}$, $\mu = 1.094 \text{ mm}^{-1}$, $R(\text{F}) = 0.0366$, $wR(\text{F}^2) = 0.0834$.

Crystallographic data have been deposited, in CIF format, with the Cambridge Crystallographic Data Centre and can be obtained, on request, from the Director, Cambridge Data Crystallographic Centre, 12 Union Road, Cambridge, CB2 1EZ, UK.

Acknowledgment. We thank the CNRS and the Région Pays de Loire for financial support to O.J.D.

Supporting Information Available: Full X-ray crystallographic data of compounds **5**, **8**, and **11**. This material is available free of charge via the Internet at <http://pubs.acs.org>.

JO000518L